doi:10.2533/chimia.2022.223 Chimia 76 (2022) 223–228

Microstructure–Property Control in Functional Materials by Multilayer Design

Claudia Cancellieri*, Giacomo Lorenzin, and Lars P. H. Jeurgens

Abstract: Smart microstructure and interface design in nanomultilayers allows to tailor physical properties like thermal stability, thermal conductivity and directional metal outflow for targeted applications. In this work, selected examples of nanomultilayer systems, constituted of alternating nanolayers of metals and/or nitrides, as precisely fabricated with variable textures, microstructures, grain sizes and internal stresses are presented. The role of the microstructure and stress state on selected functional properties is shown.

Keywords: Interface · Microstructure · Multilayers · Stress

Dr. Claudia Cancellieri is a group leader/research scientist at Empa in the Laboratory for Joining Technologies and Corrosion. In 2008 she obtained her PhD in Physics at École Polytechnique Federal in Lausanne (EPFL), specializing in Pulsed Laser Deposition growth of cuprates and oxide thin films under strain. During her first post-doc at the University of Geneva, she focused on the growth and characterization of complex oxide interfaces. She continued the investigation of this topic at the synchrotron Swiss Light Source, Paul Scherrer Institute where she extensively used spectroscopy techniques to derive the electronic band structure of buried complex oxide interfaces. Her current research topics include the investigation of microstructure, defects, stress and electronic properties of functional materials including multilayers systems.

Giacomo Lorenzin is a PhD student enrolled at the Department of Materials Science at ETH Zürich and working at Empa Dübendorf in the Laboratory for Joining Technologies and Corrosion.

He obtained his Master degree in Physics at the University of Padua in Italy in 2020 with a thesis entitled 'Low-noise mirror coatings for next-generation gravitational-wave detectors'. Currently, his research work is about metallic nanomultilayers produced with physical vapor deposition methods with a focus on the role played by interfaces in determining the stress state of the systems under investigation.

Dr. Lars Jeurgens is heading the Empa laboratory for Joining Technologies and Corrosion since 2012. He obtained his PhD in materials sciences at the Delft University of Technology (NL) in 2001. After a postdoc period working for the Dutch technology foundation (STW), he became a group leader at the Max Planck Institute for Metals Research in Stuttgart (Germany) in 2003. His research interests comprise the surface and interface engineering of metals, alloys, oxides and their coating systems for joining and corrosion management, which includes interfacial design and application of nanostructured materials for emerging micro- and nano-joining technologies.

1. Introduction

Nano-multilayers (NMLs) are functional nano-architectures,[1] consisting of a sequence of alternating nanolayers of two or more dissimilar materials, typically a metal, alloy, oxide and/or nitride. For example, nanolaminated structures of two immiscible metals (*e.g.* Cu/W, Cu/Ta), or a metal and a nitride (*e.g.* Ag/AlN,[2,3] Cu/AlN,[4] AgCu/AlN[5]), are commonly applied in microelectronics, interconnections and sensing devices. Functional NMLs offer very flexible design criteria for achieving a unique combination of mechanical,[6] magnetic, optical[7] and/or radiation-tolerant[8] properties. However, such functional NML properties are intrinsically related to their microstructure, in particular, the chemical composition, layer thickness, phase constitution, grain size, texture, stress state.[9] When the thicknesses of the alternating layers are reduced to the nanoscale, the functional properties will not only be governed by the single material layer characteristics, but in particular by the defect structure of the heterointerfaces.[10] In particular the thermal, mechanical and chemical stability of NML-based technologies critically depend on the microstructural evolution of the interfacial regions during fabrication, processing and operation, which may involve harsh environments and elevated temperatures. Thermally activated atomic rearrangements at heterointerfaces are driven by in-plane and out-of-plane gradients in the chemical potential and the stress, which can be both intrinsic (arising during growth) and extrinsic (imposed by post-treatments) in origin. On the downside, thermal annealing can induce detrimental modifications of functional heterointerfaces in electronic and optical devices. On the upside, NMLs can be transformed intentionally into nanocomposites (NC) with a desired combination of mechanical, thermal and/or electrical properties, by tuning the relative volume fraction of the constituent phases in the NML.[11] Physical Vapor Deposition (PVD) is a common technique to fabricate NMLs since it offers precise control of the chemical composition, individual layer thickness, periodicity and roughness. Not only the as-deposited NML microstructure and stress state can be controlled by careful tuning of the deposition parameters; also the interface structures can be tailored, in par-

*Correspondence: Dr. C. Cancellieri, E-Mail: claudia.cancellieri@empa.ch
Empa, Swiss Federal Laboratories for Materials Science and Technology, Laboratory for Joining Technologies and Corrosion, Überlandstrasse 129, CH-8600 Dübendorf, Switzerland.

ticular, the coherency, morphology and sharpness (atomic mixing) of the heterointerfaces. Smart microstructural design of the NML building blocks provides a powerful tool to tailor mechanical properties, electrical and thermal conductivity, as well as the thermal stability (durability) in harsh environments. However, the correlation between NML microstructure and specific functional properties is not always evident. In this contribution, several examples of smart multilayer design, by combining dissimilar materials with tuned microstructures, will be presented and correlated with their functional properties, such as thermal stability, thermal conductivity and atomic mobility (Table 1). A clear link between nanoscale interface structure and physical properties is established for these multilayers systems, which can pave the way to optimize NML microstructures for targeted applications.

Table 1. Important microstructural features which can impact resulting physical properties

Microstructure	Properties
Texture	Thermal stability
Stress	Elastic coefficient and hardness (mechanical properties)
Grain size	
Morphology	Thermal conductivity
Disorder	Surface wettability and joining
Roughness	

2. Microstructure–Properties Relationship

In this section, different examples of microstructural changes in NML systems induced by post-annealing treatments will be given, especially in dependence of the layer thickness and the intrinsic stress state. It is important to note that the isolation of the effect of individual microstructural parameters on the functional properties is very challenging and not always possible due to the strong correlation between *e.g.* the texture, grain size, layer thickness and stress state.

2.1 *Effect of the High-temperature Annealing*

The phase stability of confined metals in nanomultilayer structures can be severely compromised by high-temperature annealing. From a thermodynamic viewpoint, the presence of multiple internal interfaces (*i.e.* heterointerfaces and grain boundaries), as associated with excess Gibbs energies and strain, makes the multilayer prone to degradation. From a kinetic viewpoint, these internal interfaces can act as short-circuit diffusion paths, thus providing relatively fast atom mobilities at reduced temperatures as compared to the respective bulk materials. For example, immiscible Cu/W multilayers undergo a multilayer degradation upon heating at T >750 °C, forming a Cu-W nanocomposite.[12] At this temperature, the ordered periodic Cu/W NML structure with specific in-plane and out-of-plane crystallographic orientations is replaced by a nanocomposite of W particles embedded in a Cu matrix. This temperature coincides also with complete stress relaxation of W,[13] which runs in parallel with the relaxation of the interface stresses.[14] Notably, the Cu phase already relaxes its stress at much lower temperatures (T ~500 °C) by outflow to the NML surface (Fig. 1), especially if the NMLs are previously irradiated with an ion-beam to increase the defect concentration and stress level.[15] The kinetics of Cu/W multilayer degradation upon thermal annealing has been investigated by *in situ* high temperature XRD.[12] It was found that the mobility of Cu and W atoms is important in different stages of the NML degradation process. Delamination proceeds by grain boundary grooving, which is rate-limited by the atomic mobility of W along Cu/W heterointerfaces and/or W grain boundaries. The onset temperature for the degradation depends strongly on the multilayer microstructure, in particular, the individual layer thicknesses and the processing atmosphere.[16] Strikingly, in Ag/AlN NMLs, a processing atmosphere with small amounts of oxygen triggers massive Ag outflow to the NML surface at temperatures as low as 400 °C, whereas in vacuum such Ag outflow is negligible.[3] In all studied NML systems (as prepared by magnetron sputtering), the coherency and atomic roughness of the (defective) heterointerfaces is enhanced upon short time annealing at intermediate temperatures, well below the onset temperature for NML degradation. The reduction of the interface energies, the chemical interaction with oxygen, as well as the relaxation of stresses, constitute the main driving forces for the thermal degradation of NML systems.

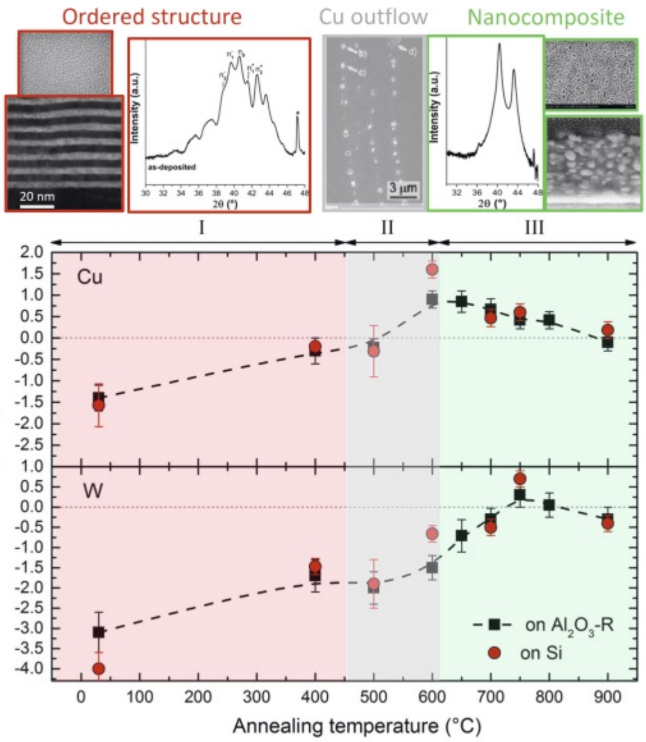

Fig. 1. Stress evolution upon *ex situ* annealing in Cu/W nanomultilayers as derived by XRD analysis. Three stages of the microstructural evolution are identified: 1. Preservation of an ordered periodic structure up to 400 °C, 2. Cu surface migration at 400 < T < 600 °C, 3. Transformation into Cu-W nanocomposite at T > 750 °C. Adapted from ref. [13].

2.2 *Effect of the Layer Thickness*

As a rule of thumb, the average grain size approximately scales with the individual layer thickness for film thicknesses in the nanometer range.[12] So changing the Cu and W layer thicknesses is likely to change the grain size of the individual NML blocks. The thermal stability of Cu/W NMLs is higher for a bilayer unit 10-nm-W/10-nm-Cu as compared to a respective bilayer unit with a smaller W layer thickness. For 10-nm-W/10-nm-Cu NMLs the periodic structure is preserved until T = 800 °C.[16] The W layers reach a stress-free state only after complete transformation into a nanocomposite. The initial compressive stresses in the Cu nanolayers are relaxed at lower temperatures (before the onset of the delamination process) by surface outflow, as governed by the initial layer thicknesses (Fig. 2). The individual layer thicknesses determine the magnitude of the initial compressive stress states in Cu and W, thus providing an important tool for stress tailoring in Cu/W NMLs.[16] A recent study on the effect of the cosputtered Cu/W period on the thermal stability has shown that larger bilayer

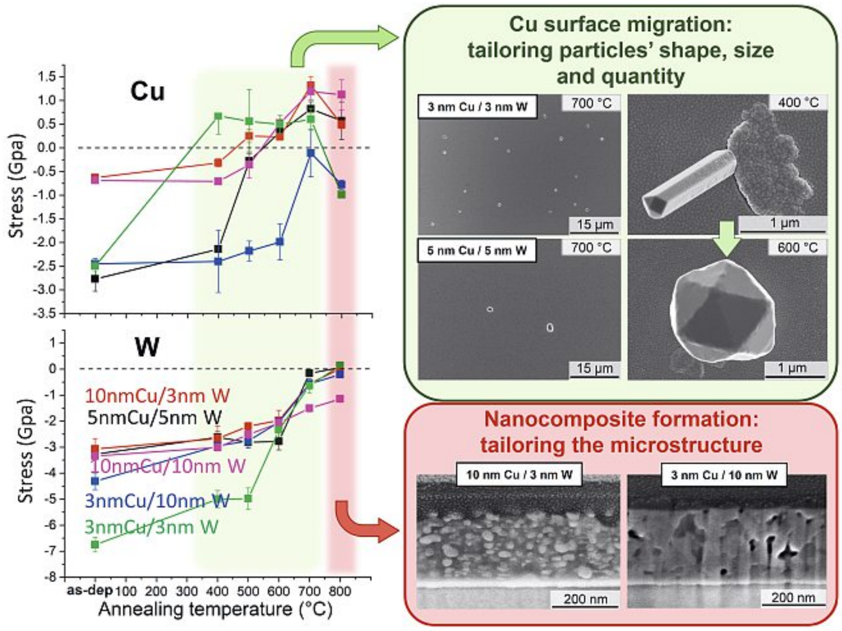

Fig. 2. Dependence of the individual layer thickness of Cu and W on the stress evolution in Cu/W NMLs upon annealing. A complete destruction of the nanolaminated structure occurs at 800 °C, as associated with the formation of a Cu-W nanocomposite. The resulting nanocomposite microstructure depends on the initial Cu and W layer thicknesses. Adapted from ref. [16].

periods (~27 nm) result in a higher resistance against thermal degradation, as attributed to the improved diffusion barrier properties of thicker W-rich layers.[17] Cu-W bilayers with an intermediate bilayer thickness between 7 and 14 nm maintain the highest hardness upon high-temperature annealing, indicating the significant role of the bilayer period on high-temperature mechanical stability.

Moreover, Cu-W multilayers with a period thickness up to 12 nm were found to be highly resistant against ion beam irradiation.[18] In metal/ceramic Ag/AlN, Cu/AlN and Ag-Cu/AlN NMLs, significant microstructural changes are already observed at much low temperatures around 300 °C.[19] For AlN barrier thicknesses ≥8 nm, interconnected line-shape protrusions of Cu appear at the NML surface upon annealing, as attributed to the thermal-mismatch-induced fracturing of the brittle AlN barrier layers. The microstructure and internal stresses in the AlN barrier layers clearly play an important role in determining the thermal-mismatch-induced fracture pattern and thereby the arrangement of metal protrusions on the annealed NML surface. For AlN thicknesses of 4 nm, the AlN barrier behaves much more ductile, resulting in the appearance of Cu and Ag spherical surface protrusions upon annealing (Fig. 3). For these very thin AlN barrier layers, the AlN nanograins have not yet completely coalesced in a continuous and dense barrier layer structure. Consequently, the AlN barrier layer rather behaves as a flexible nanoporous membrane (*i.e.* thermal-mismatch-induced fracturing is not observed); the open grain boundary structure provides an easy pathway for the outflow of Ag-Cu across the AlN nanolayer towards the outer surface.

Open grain boundaries, nanopores and controlled localized deformation of NMLs by nanoindentation[20] provide alternative pathways for controlling and patterning metal outflow from NMLs upon rapid annealing, which could be exploited for localized bonding and simultaneous interconnecting of micro- or nano-scaled object at patterned NML surfaces. Other factors, like oxygen in the atmosphere and internal stress relaxation may also favor the directional diffusion of the confined metal phase.[3]

2.3 *Effect of the Strain Gradient*

As shown above, internal stress is responsible for mechanical and thermal instabilities, which can lead to failure and reliability issues in NMLs.[21] The main challenge is that the stress distribution is not homogeneous across the NML depth and therefore the presence of a strain/stress gradients cannot be neglected.[22] The assessment of strain depth profiles in thin films and multilayers in the nanometer range is not straightforward and requires advanced XRD analysis combined with a specific measurement geometry.[23] Important stress contributions typically occur in the vicinity of internal heterointerfaces, as well as at the main interfaces of the NML with parent substrate and the free surface. In general, buried layers in the vicinity of the incoherent interface with a crystalline substrate will experience higher strains than top

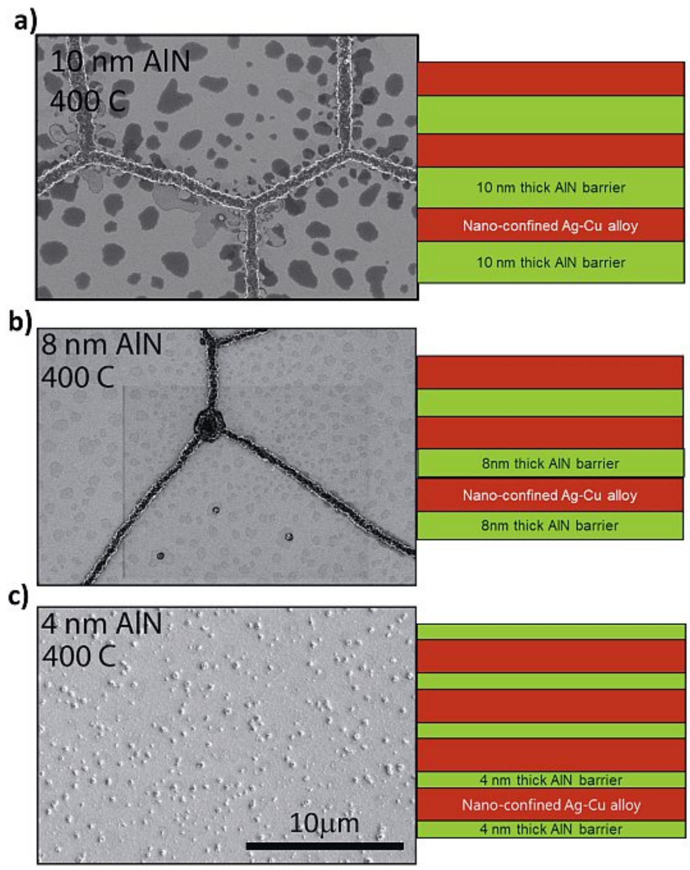

Fig. 3. Planar SEM images of Ag-Cu/AlN nanomultilayers after 400 °C annealing in air. Different sizes and shapes of Cu and/or Ag protrusions appear on the annealed NM surface, depending on the AlN barrier thickness. Adapted from ref. [19].

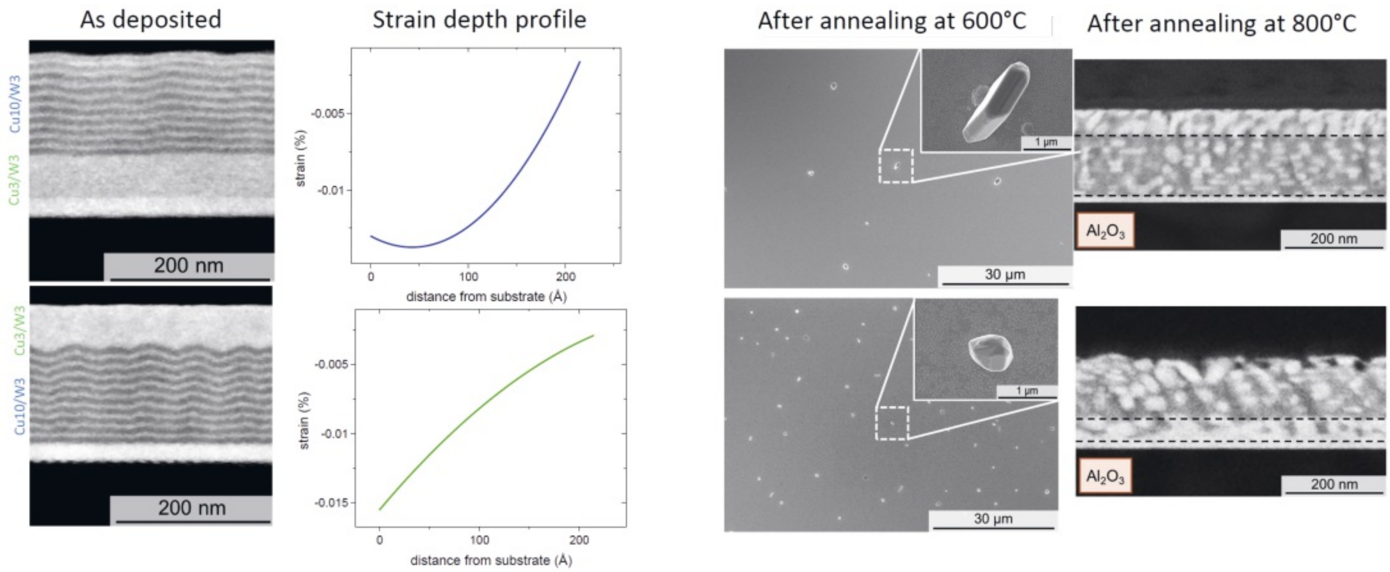

Fig. 4. Graded Cu/W nanomultilayers as obtained by combining two different bilayer stacks. The different as-deposited strain depth profiles result in different Cu outflow patterns after annealing at 600 °C, as well as in differently graded nanocomposite microstructures after annealing at 800 °C. Adapted from ref. [24].

layers adjacent to the free surface, since growth stresses can more easily relax towards the free surface. For example, for single Cu layers deposited on sapphire substrates, a combination of coherency and depositon stresses occur in the first few nanometers adjacent to the substrate, which is gradually relaxed towards the film surface.[23] For NML systems, different strain depth distributions can be obtained by varying the bilayer thickness across the depth. For example, different stress gradients in Cu/W NML were obtained by varying the sequence of the bilayer building blocks.[24] Noteworthy, the average internal stress derived by conventional XRD was found to be very similar for both NML systems and is therefore blind to distinguish such in-depth strain gradients.[24] The amount of Cu outflow upon annealing of these two differently stacked Cu/W NMLs (in the range of 400–600 °C) was found to depend on the shape of the strain profile; this suggests that smart design of the bilayer block arrangement might be exploited as a tool to tailor surface outflow of the confined metal. Comparison with strain depth profiles of single layers of W and Cu with a similar thickness (~200 nm) clearly evidences that multilayer design provides a powerful tool for tailoring in-depth stress gradients. Moreover, the nanocomposite microstructure, as obtained after NML degradation at 800 °C, also has a differently graded compositional structure in depth, depending on the sequence of the different bilayer stacks (Fig. 4).

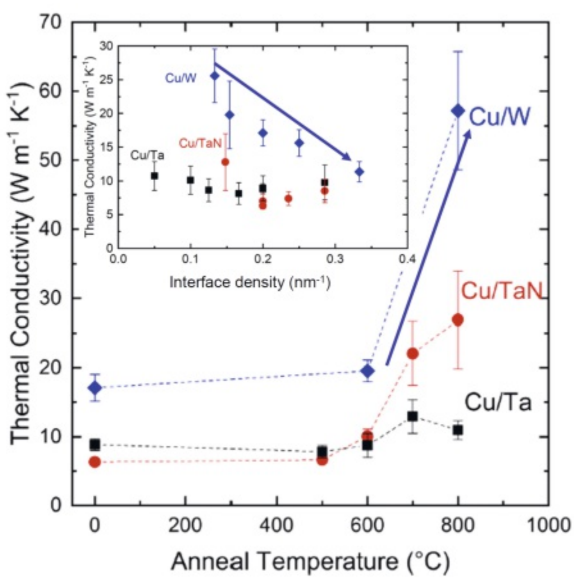

Fig. 5. Thermal conductivity evolution as function of the interface density (inset) and as function of the annealing temperature for different Cu-based multilayers. Adapted from ref. [28].

2.4 *Effect of the Interface*

Heterointerfaces in multilayers determine the chemical adherence, coherency, interface stress, structural stability and interfacial atom mobility under harsh processing and/or operating conditions. Incoherent (defective) heterointerfaces between two chemically inert crystalline solids can promote interfacial pre-melting (resulting in a melting point depression; MPD) and offer an enhanced interfacial atomic mobility. In contrast, coherent (epitaxial) heterointerfaces between two chemically inert crystalline solids generally obstruct interfacial pre-melting (causing superheating) and suppress interfacial atomic mobility. Model predictions of Ag/AlN and Cu/AlN interface structures by DFT evidence that the semi-coherent Cu/AlN interface contains a higher density of lattice misfit dislocations and/or point defects[25] than the more coherent Ag/AlN interface.

The atomic mobility of Cu along the semi-coherent Cu/AlN interface is therefore considerably higher as compared to the atomic mobility of Ag along the Ag/AlN interface. This facilitates transport of Cu along internal Cu/AlN interfaces to defective sites (*i.e.* permeable channels) in the AlN barrier layers for patterned surface outflow by rapid thermal annealing.[4] Doping of Ge at the AlN interface of Ag/AlN NMLs effectively suppresses Ag outflow upon annealing; Ag outflow then occurs mainly through thermal-mismatch-induced cracking of the barrier layer.[26] Interfacial Ge also changes the stress state in Ag from compressive to tensile. In the presence of Ge, the interfaces become more ordered after annealing,[27] thus improving the thermal stability of the system.

Thermal conductivity in NML has been found to mainly depend on the interface density.[28] Interfacial thermal resistance is the primary impediment to heat flow in materials and devices, as characteristic lengths become comparable to the mean-free paths of the energy carriers. In Cu/W multilayers, thermal conductivity was found to inversely scale with the interface density (inset

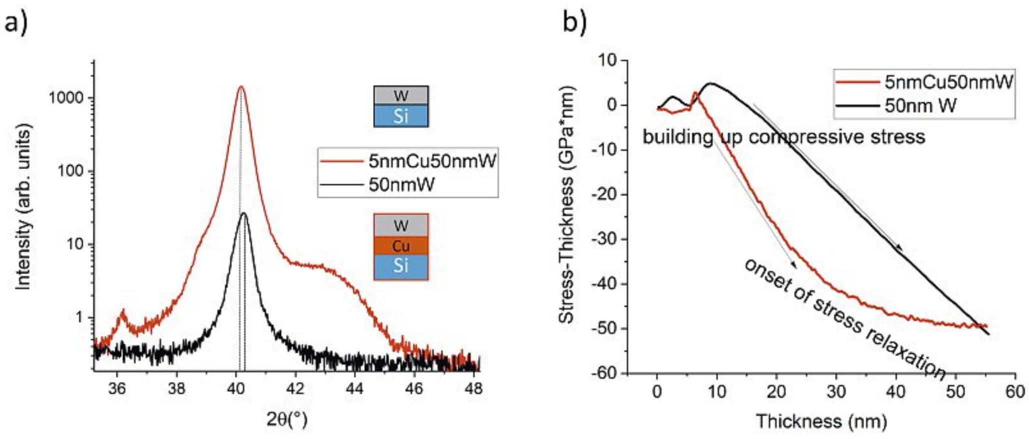

Fig. 6. a) XRD pattern of a 50-nm-thick W layer grown on a Si substrate with and without a 5 nm Cu buffer layer. b) Stress-thickness curve measured during the growth of the different heterostructures.

Fig. 5), while in other systems, like Cu/Ta and Cu/TaN, the effect is less pronounced. The resistance between adjacent layers within a period depends not only on the material combination, but also on the structural disorder at the heterointerfaces. The thermal conductivity of Cu/W NMLs is thus boosted by the reduction of internal interfaces, as induced by *e.g*. NML degradation and NC formation upon high temperature annealing (Fig. 5).

The characteristics of heterointerfaces in NML systems also affect the grain size and disorder of the alternating nanolayers. A different parent substrate changes the atomic structure of the substrate/multilayer interface, resulting in a different stress state and crystalline quality of the NML stack. For example, 50 nm of W deposited on a Si substrate with and without a 5-nm-thick Cu interlayer results in very different microstructures and stress states (see Fig. 6a). The XRD intensity of the W(110) reflection is 2 orders of magnitude more intense in the presence of a 5-nm-thick Cu interlayer between the Si substrate and the W layer. The resulting internal stress is also very different with and without the Cu interlayer (see the peak shift in Fig. 6a). The stress evolution during growth, as measured by *in situ* curvature method, indicates that the relaxation of accumulated compressive growth stresses in W is facilitated in the presence of a thin Cu interlayer (Fig. 6b). These findings indicate the major role played by the substrate/overlayer interface in determining the microstructure and stress state of single and multilayer systems.

3. Conclusions

The impact of the microstructure on the physical properties of functional materials by multilayer design has been briefly exemplified. The comprehensive understanding of the property–microstructure relationship requires accurate control of the atomic structure and composition of the heterointerfaces, the individual layer thicknesses, as well as the in-depth stress gradients. The delicate interplay between the above microstructural features determines the functional properties, reliability and durability of material heterostructures, not only in their as-grown condition, but also upon operation under harsh conditions, which is of utmost important for real-life applications.

Acknowledgements

The authors acknowledge all the staff of the Laboratory for Joining Technologies and corrosion for their constant support. G. Lorenzin acknowledges the Swiss National Science Foundation (SNSF project number 200021_192224) for financial support.

Received: January 26, 2022

[1] S. J. Lloyd, J. M. Molina-Aldareguia, *Phil. Trans. Roy. Soc. London A* **2003**, *361*, 2931, https://doi.org/10.1098/rsta.2003.1276.
[2] A. Siozios, N. Kalfagiannis, D. V. Bellas, C. Bazioti, G. P. Dimitrakopulos, G. Vourlias, W. M. Cranton, E. Lidorikis, D. C. Koutsogeorgis, P. Patsalas, *Nanotechnology* **2015**, *26*, 155301, https://doi.org/10.1088/0957-4484/26/15/155301.
[3] M. Chiodi, C. Cancellieri, F. Moszner, M. Andrzejczuk, J. Janczak-Rusch, L. P. H. Jeurgens, *J. Mater. Chem. C* **2016**, *4*, 4927, https://doi.org/10.1039/C6TC01098A.
[4] J. Janczak-Rusch, M. Chiodi, C. Cancellieri, F. Moszner, R. Hauert, G. Pigozzi, L. P. H. Jeurgens, *Phys. Chem. Chem. Phys*. **2015**, *17*, 28228, https://doi.org/10.1039/C5CP00782H.
[5] J. Janczak-Rusch, M. Chiodi, C. Cancellieri, F. Moszner, R. Hauert, G. Pigozzi, L. P. H. Jeurgens, *Phys. Chem. Chem. Phys.* **2015**, *17*, 28228, https://doi.org/10.1039/c5cp00782h.
[6] B. M. Clemens, H. Kung, S. A. Barnett, *MRS Bull*. **2013**, *24*, 20, https://doi.org/10.1557/S0883769400051502.
[7] C. D. Appleget, A. M. Hodge, *Opt. Mater. Express* **2020**, *10*, 850, https://doi.org/10.1364/OME.389156.
[8] Y. Gao, T. Yang, J. Xue, S. Yan, S. Zhou, Y. Wang, D. T. K. Kwok, P. K. Chu, Y. Zhang, *J. Nucl. Mater.* **2011**, *413*, 11, https://doi.org/10.1016/j.jnucmat.2011.03.030.
[9] A. Sáenz-Trevizo, A. M. Hodge, *Nanotechnology* **2020**, *31*, 292002, https://doi.org/10.1088/1361-6528/ab803f.
[10] A. I. Fedorenko, Y. P. Pershin, O. V. Poltseva, A. G. Ponomarenko, D. L. Voronov, S. A. Yulin, *MRS Proc*. **2011**, *458*, 249, https://doi.org/10.1557/PROC-458-249.
[11] T. E. Twardowski, 'Introduction to nanocomposite materials : properties, processing, characterization', DEStech Publications, Lancaster, **2007**.
[12] F. Moszner, C. Cancellieri, M. Chiodi, S. Yoon, D. Ariosa, J. Janczak-Rusch, L. P. H. Jeurgens, *Acta Mater.* **2016**, *107*, 345, https://doi.org/10.1016/j.actamat.2016.02.003.
[13] C. Cancellieri, F. Moszner, M. Chiodi, S. Yoon, J. Janczak-Rusch, L. P. H. Jeurgens, *J. Appl. Phys*. **2016**, *120*, 195107, https://doi.org/10.1063/1.4967992.
[14] A. V. Druzhinin, C. Cancellieri, L. P. H. Jeurgens, B. B. Straumal, *Scripta Mater*. **2021**, *199*, 113866, https://doi.org/10.1016/j.scriptamat.2021.113866.
[15] L. Romano Brandt, E. Salvati, D. Wermeille, C. Papadaki, E. Le Bourhis, A. M. Korsunsky, *ACS Appl. Mater. Interf*. **2021**, *13*, 6795, https://doi.org/10.1021/acsami.0c19173.
[16] A. V. Druzhinin, D. Ariosa, S. Siol, N. Ott, B. B. Straumal, J. Janczak-Rusch, L. P. H. Jeurgens, C. Cancellieri, *Materialia* **2019**, *7*, 100400, https://doi.org/10.1016/j.mtla.2019.100400.
[17] J. Xue, Y. Li, L. Gao, D. Qian, Z. Song, X. Wang, X. Zhu, J. Chen, *Surf. Coat. Technol*. **2020**, *381*, 125179, https://doi.org/10.1016/j.surfcoat.2019.125179.
[18] L. Dong, H. Zhang, H. Amekura, F. Ren, A. Chettah, M. Hong, W. Qin, J. Tang, L. Hu, H. Wang, C. Jiang, *J. Nucl. Mater*. **2017**, *497*, 117, https://doi.org/10.1016/j.jnucmat.2017.07.064.
[19] V. Araullo-Peters, C. Cancellieri, M. Chiodi, J. Janczak-Rusch, L. P. H. Jeurgens, *ACS Appl. Mater. Interf.* **2019**, *11*, 6605, https://doi.org/10.1021/acsami.8b19091.
[20] L. Lin, L. P. H. Jeurgens, *ACS Appl. Mater. Interf.* **2019**, *11*, 39046, https://doi.org/10.1021/acsami.9b10498.
[21] J. L. Beuth, S. H. Narayan, *Int. J. Solids Struct.* **1996**, *33*, 65, https://doi.org/10.1016/0020-7683(95)00021-2.
[22] L. Romano-Brandt, E. Salvati, E. Le Bourhis, T. Moxham, I. P. Dolbnya, A. M. Korsunsky, *Surf. Coatings Technol.* **2020**, *381*, 125142, https://doi.org/10.1016/j.surfcoat.2019.125142.
[23] C. Cancellieri, D. Ariosa, A. V. Druzhinin, Y. Unutulmazsoy, A. Neels, L. P. H. Jeurgens, *J. Appl. Crystallogr*. **2021**, *54*, 87, https://doi.org/10.1107/S1600576720014843.

[24] A. V. Druzhinin, G. Lorenzin, D. Ariosa, S. Siol, B. B. Straumal, J. Janczak-Rusch, L. P. H. Jeurgens, C. Cancellieri, *Mater. Design* **2021**, *209*, 110002, https://doi.org/10.1016/j.matdes.2021.110002.
[25] G. Pigozzi, A. Antušek, J. Janczak-Rusch, M. Parlinska-Wojtan, D. Passerone, C. A. Pignedoli, V. Bissig, J. Patscheider, L. P. H. Jeurgens, *Appl. Phys. Lett*. **2012**, *101*, 181602, https://doi.org/10.1063/1.4761471.
[26] C. Cancellieri, E. Klyatskina, M. Chiodi, J. Janczak-Rusch, L. P. H. Jeurgens, *Appl. Sci*. **2018**, *8*, 2403, https://doi.org/10.3390/app8122403.
[27] D. Ariosa, C. Cancellieri, V. Araullo-Peters, M. Chiodi, E. Klyatskina, J. Janczak-Rusch, L. P. H. Jeurgens, *ACS Appl. Mater. Interf.* **2018**, *10*, 20938, https://doi.org/10.1021/acsami.8b02653.
[28] C. Cancellieri, E. A. Scott, J. Braun, S. W. King, R. Oviedo, C. Jezewski, J. Richards, F. L. Mattina, L. P. H. Jeurgens, P. E. Hopkins, *J. Appl. Phys*. **2020**, *128*, 195302, https://doi.org/10.1063/5.0019907.